

Cite this: *J. Mater. Chem. A*, 2018, 6, 5260Received 4th August 2017
Accepted 13th September 2017

DOI: 10.1039/c7ta06883b

rsc.li/materials-a

Gaodefroyite: a mineral with excellent magnetocaloric effect suitable for liquefying hydrogen

Rukang Li,^{ab} Guangjing Li^c and Colin Greaves^{id}*^c

Gaodefroyite contains chains of edge-linked MnO_6 octahedra on a Kagomé lattice which results in magnetic frustration between the chains and overall spin-liquid behaviour below 9 K. Magnetization and specific heat measurements indicate very large entropy increases for temperatures of 10–30 K on removal of applied magnetic fields as low as 2 T. This is attributed to the degenerate magnetic ground states originating from the frustrated Kagomé lattice. Direct temperature change measurements confirm that the mineral has excellent low-field magnetocaloric properties suitable for refrigeration to produce liquid hydrogen.

Magnetocaloric (MC) refrigeration is both energy-efficient and environmentally friendly:^{1,2} energy efficiencies > 50% are theoretically achievable (*cf.* 35% for compressor-based systems) with no risk from greenhouse gases. Although materials with enhanced MC effect (MCE) are still needed for more efficient domestic refrigeration^{3,4} and to achieve extremely low temperatures, *e.g.* for space exploration,⁵ their advantages have more recently been considered for producing liquid hydrogen (LH_2 , b.p. 20 K)^{6,7} for fuel storage in a clean hydrogen economy.⁸ Unfortunately, known MC materials do not meet the requirements of efficiency and chemical stability while operating at low magnetic fields (2 T), and no other methods, *e.g.* thermoelectric cooling, are efficient in this temperature range. The mineral gaodefroyite has magnetic features which have signposted a possible solution to these problems, and here we report results which support its unique properties.

The MCE results from the increase in magnetic entropy of a magnetic material when an external magnetic field is removed. Under adiabatic conditions, the temperature falls to maintain a constant overall entropy. Efficient MC refrigeration

requires a large change in magnetic entropy, which has traditionally been achieved with paramagnetic ions with very large effective moments such as Gd^{3+} ($S = J = 7/2$). However, a serious problem for producing LH_2 in this way is the reduction in MCE at temperatures of ~ 20 K for such materials (*e.g.* gadolinium gallium garnet (GGG), GdPO_4) or the more recently proposed molecular magnets.^{9,10} The metallic ferromagnetic (FM) and the “giant” MC intermetallic materials^{11,12} are also unsuitable because of long term degradation in contact with LH_2 .⁶ Although Dy-doped GGG (or the aluminium analogue (GAG)) show useful characteristics, their need for a superconducting magnet to generate magnetic fields of 6 T restricts their applicability.^{6,13} Various proposals to increase the MCE at fields that can be generated by permanent magnets (~ 2 T) have been reported, in particular the use of FM intermetallics that have a first order structural transition and display giant MCE behavior.^{3,4,14} However, these materials are limited by their small operating temperature range and energy inefficiency. Reducing the magnetic interaction to one-dimension (1D)¹⁵ or even zero-dimension (0D)¹⁶ and employing magnetic frustration have also been proposed. With respect to frustration, theoretical predictions suggested enhanced MCE in geometrically frustrated spin systems with Kagomé, garnet and pyrochlore lattices or even molecular systems because of the large entropy provided by the highly degenerate magnetic ground states in zero field.^{17,18} Importantly, the MCE was predicted to give very rapid cooling for fields providing near magnetic saturation, which was subsequently confirmed for the pyrochlore structure.¹⁹

Our previous study of the mineral gaodefroyite, $\text{Ca}_4\text{Mn}_3\text{O}_3(\text{BO}_3)_3\text{CO}_3$, and its synthetic analogue $\text{YCa}_3\text{Mn}_3\text{O}_3(\text{BO}_3)_4$, revealed interesting magnetic features that suggested the possibility for enhanced MC properties. Both materials contain 1D chains of Mn^{3+} ions^{20,21} and, at low temperatures, the Mn magnetic moments in any given chain display FM order. Extended linear clusters of FM-coupled moments can simulate a system with “giant” spins. However, the chains are located on a Kagomé lattice that inhibits 3D magnetic order. MCE

^aBeijing Centre for Crystal Research and Development, Key Laboratory of Functional Crystals and Laser Technology, Technical Institute of Physics and Chemistry, Chinese Academy of Sciences, Beijing 100190, P. R. China. E-mail: rkli@mail.ipc.ac.cn

^bUniversity of Chinese Academy of Sciences, Beijing 100049, P. R. China

^cSchool of Chemistry, University of Birmingham, Birmingham B15 2TT, UK. E-mail: c.greaves@bham.ac.uk



enhancement is expected from both the giant spins and also from the frustration preventing interchain order. The co-operative effects could therefore provide very rapid cooling rate with high MCE for a stable material free from expensive rare earth elements.

Gaodefroyite is found in hydrothermal manganese deposits and good crystals (Fig. 1(a) and (b)) can be found in South Africa.²² The hexagonal structure^{23,24} has 1D chains of edge-shared, Jahn–Teller distorted MnO₆ octahedra aligned along [001] and linked by BO₃ groups (Fig. 1(c)); in the *ab* plane, the chains define a 2D Kagomé net. The hexagonal channel of the net hosts Ca²⁺ ions and CO₃ groups; additional Ca²⁺ ions sit in the smaller trigonal channels. The FM MnO₆ chains experience antiferromagnetic exchange within the *ab* plane but the inherent frustration gives different magnetic structures for the mineral and YCa₃Mn₃O₃(BO₃)₄. In the latter, the moments order below 7.5 K into a *q* = 0 Kagomé type magnetic structure (Fig. 1(d)) but in gaodefroyite itself, the moments freeze to a spin-liquid state. The difference is an example of order by disorder – the disordered Y/Ca sublattice in YCa₃Mn₃O₃(BO₃)₄ promotes magnetic order. The spin-liquid state with large density of unfrozen entropy stimulated us to study the MCE of natural gaodefroyite.

The mineral samples used in our study were from Wessels Mine, Kalahari Manganese Field, Northern Cape Province, South Africa, with hexagonal prism shaped crystals of typical size 6 × 7 × 21 mm³ (Fig. 1(a)). The crystals were cut to provide 3 × 1 × 4 mm³, 4.6 × 2.5 × 6 mm³ (Fig. 1(b)) and 2.4 × 4.1 × 5.8 mm³ crystals for different measurements. X-ray fluorescence analyses showed that the raw crystal contained only minor impurities of Cl (1.2%), Si (0.26%), Fe (0.21%) and S (0.15%).

GdCa₃Mn₃O₃(BO₃)₄ was synthesised using the method previously described: pure Gd₂O₃, CaCO₃, MnO₂ and H₃BO₃ were heated in air initially at 600 °C for 10 h and subsequently

for three periods of 24 h at 1050 °C.²¹ Magnetic and specific heat data were collected from a Quantum Design PPMS magnetometer using the oriented crystals with size of 3 × 1 × 4 mm³ for gaodefroyite and a sintered pellet for GdCa₃Mn₃O₃(BO₃)₄.

Field dependent magnetisations in gaodefroyite at temperatures below 15 K with the field applied perpendicular to [001] revealed a sharp increase in magnetisation to >60% of its saturated value with a field of only 2 T (Fig. 2(a)), indicative of a large MCE effect at small field. The entropy changes calculated from the magnetisation curves,²⁵ Fig. 2(b), show a maximum value of |Δ*S*| ≈ 7 J kg^{−1} K^{−1} at 11 K for a field of 2 T and agree with those from integration of the specific heats²⁵ at 0 and 2 T, Fig. 2(c). Fig. 2(b) also compares Δ*S* data with those at the same field for Gd(HCOO)₃.⁹ Whereas Δ*S* for gaodefroyite remains > 3 J kg^{−1} K^{−1} for temperatures of 6–24 K, *i.e.* suitable for LH₂ production, the paramagnetic Gd salt is excellent at very low temperatures but significantly inferior above ~10 K. Fig. 3(a) shows that for a field of 7 T, the entropy change increases to 15 J kg^{−1} K^{−1}. Importantly, these entropy changes are already very close to those for giant MCE behavior in some intermetallic FM materials,^{11,12} and for the best Dy- or Fe-doped gadolinium garnets – we stress that gaodefroyite contains no rare earth ions. It should be noted that despite the anisotropy, Fig. 2(b), the properties of a powder-averaged, sintered sample would also be excellent.

Direct temperature change was recorded with a thermocouple glued on one side of the gaodefroyite crystal of size 2.4 × 4.1 × 5.8 mm³ and with the other side glued on a 2 mm thick copper plate attached to the base of a cryostat (Quantum Design with optic option and a magnet of maximum field 760 mT). Data collected at ~15 K, Fig. 3(b), show that Δ*T* = −0.96 K for a field of 750 mT. The expected adiabatic temperature change, *T*_{ad} can be estimated from the crude approximation:²⁶

$$T_{\text{ad}}(T_i, H_f, H_i) = -\frac{T_i}{C_H(T_i, H_f)} \Delta S(T_i, H_f, H_i)$$

with *T*_i = 15 K, Δ*S* = −0.37 J mol^{−1} K^{−1} (estimated from Fig. 3(a), 1 kg = 4.92 mol (Mn)) and *C*_H = 5 J mol^{−1} K^{−1} (Fig. 2(c)), a temperature change of −1.1 K is predicted for this field, in good agreement with the observed value. Extrapolating to higher fields, we predict that *T*_{ad} = −3.6 K and −9 K for fields of 2 and 7 T, respectively. Even at 30 K, the temperature change will still be −1.5 K for a single cycle at 2 T. More importantly the temperature change is almost instantaneous and occurs in 60 ms, close to the limit of our temperature sampling interval of 50 ms, and much faster than the field ramp rate of 1.5 T s^{−1}. This very fast cooling rate is consistent with the theoretical prediction¹⁷ that spin frustration may enhance the cooling rate by orders of magnitude.

For the practical application of MC refrigeration, a more important parameter, the relative cooling power (RCP) defined as the product of maximum entropy change (Δ*S*) and full width at half maximum of the Δ*S*_M – *T* curve, is often used to evaluate cooling power of different MC materials. For gaodefroyite, we found RCP > 100 J kg^{−1} for the field change of 0–2 T, which is the highest among similar compounds at this field and temperature range.²⁷ This strong enhancement of RCP, due to high Δ*S*_M being spread over a large temperature range, was also

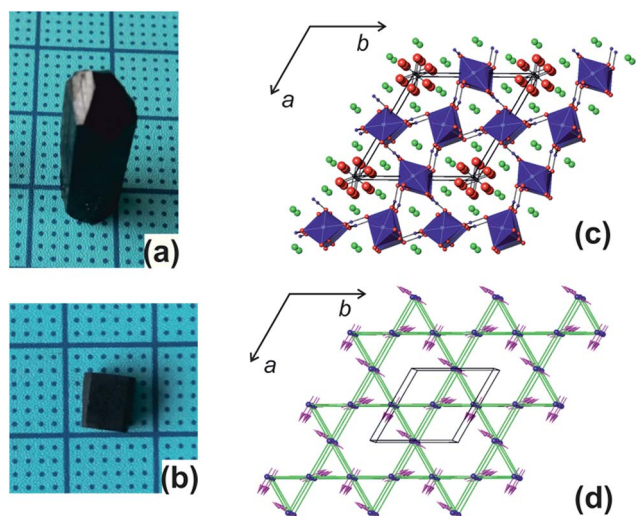


Fig. 1 (a) Crystal of gaodefroyite as obtained and (b) cut/polished with the size of 4.6 × 2.5 × 6 mm³ (*a* × *b* × *c*). (c) Crystal structure viewed approximately along [001] and showing the unit cell: the chains of MnO₆ octahedra are blue, Ca green, C black, B blue and O red. (d) The magnetic Kagomé lattice of the chains of Mn³⁺ ions (blue spheres) and the magnetic order in YCa₃Mn₃O₃(BO₃)₄.²¹



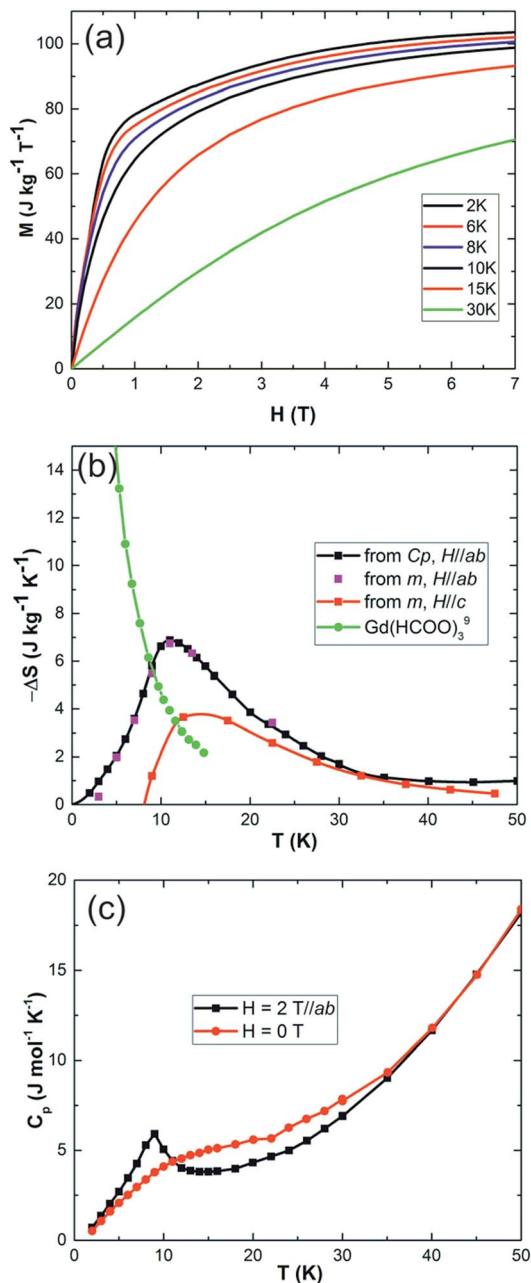


Fig. 2 (a) Low temperature isothermal magnetization of gaufreyite within the easy plane, *ab*. (b) Entropy changes of gaufreyite for a field of 2 T obtained from the magnetisation (*m* in legend) and specific heat (C_p in legend) measurements; the data are compared with those for $\text{Gd}(\text{HCOO})_3$.⁹ (c) Specific heat of gaufreyite under zero field and a magnetic field of 2 T (in the *ab* plane).

observed in the spin glass systems of Gd_2NiSi_3 and Er_2NiSi_3 and was attributed to the spin frustration.²⁷

In an actual MC refrigerator, especially with active magnetic regeneration (AMR) cycles, several pre-requisites are demanded for the MC materials:^{2,28} (1) a large entropy change at the relevant temperature for a field less than 2 T; (2) a large thermal conductivity for efficient heat exchange between the MCE material and cooling media; (3) low magnetic or structural hysteresis and high electronic resistance for reducing AC

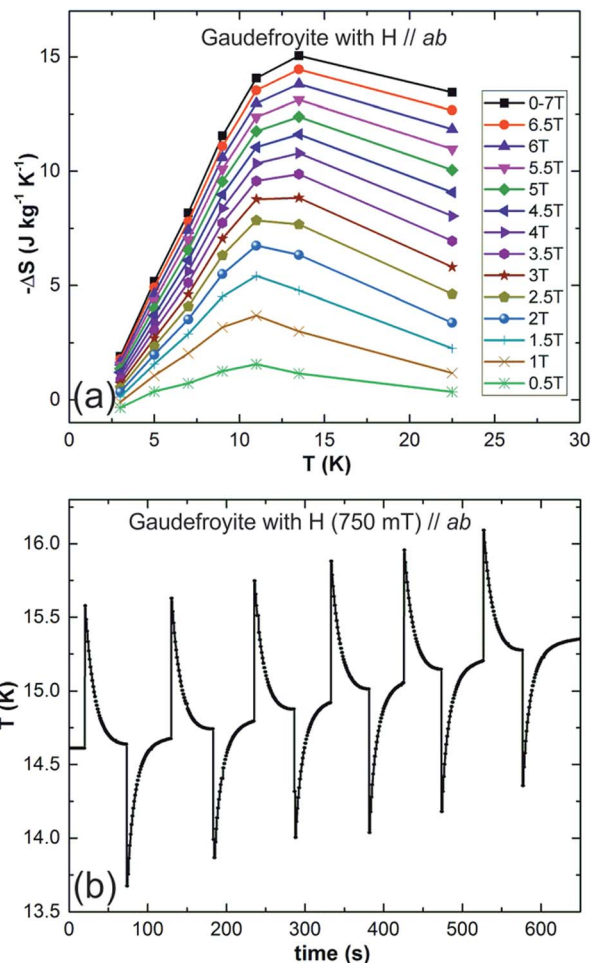


Fig. 3 (a) Entropy changes as a function of temperature for fields of 0.5 to 7 T for gaufreyite and (b) temperature change of gaufreyite on applying and removing a field of 750 mT.

operation loss²⁹ and (4) high chemical stability in contact with the cooling media (*e.g.* LH_2).

Thermal conductivity (κ) measurements (steady heat flow method³⁰ on the oriented crystal $4.6 \times 2.5 \times 6 \text{ mm}^3$) are shown in Fig. 4(a). Along *c*, κ is about $10 \text{ W m}^{-1} \text{ K}^{-1}$ for most of the temperature range examined, with a maximum of $14 \text{ W m}^{-1} \text{ K}^{-1}$ at 42 K; it drops to $3 \text{ W m}^{-1} \text{ K}^{-1}$ at 5 K. Although the thermal conductivity is an order of magnitude smaller than GGG single crystals or high purity metals, it is similar to sintered ceramics or pressed pellets,³⁰ which are generally used in MC refrigerators. Gaufreyite shows no magnetic order down to 2 K, but a spin-liquid forms below 9 K and gives a small hysteresis of 180 Oe at 1.8 K, Fig. 4(b).²⁰ The hysteresis disappears above 9 K, which is excellent for producing LH_2 at 20 K. We expect that for this application, gaufreyite will show high stability as do other oxide MC materials.

Gaufreyite therefore has excellent, low temperature MC properties and is, in fact, unique in simultaneously displaying:

(1) Strong, low field MCE ($H < 2 \text{ T}$), due to the giant spins on the MnO_6 chains;



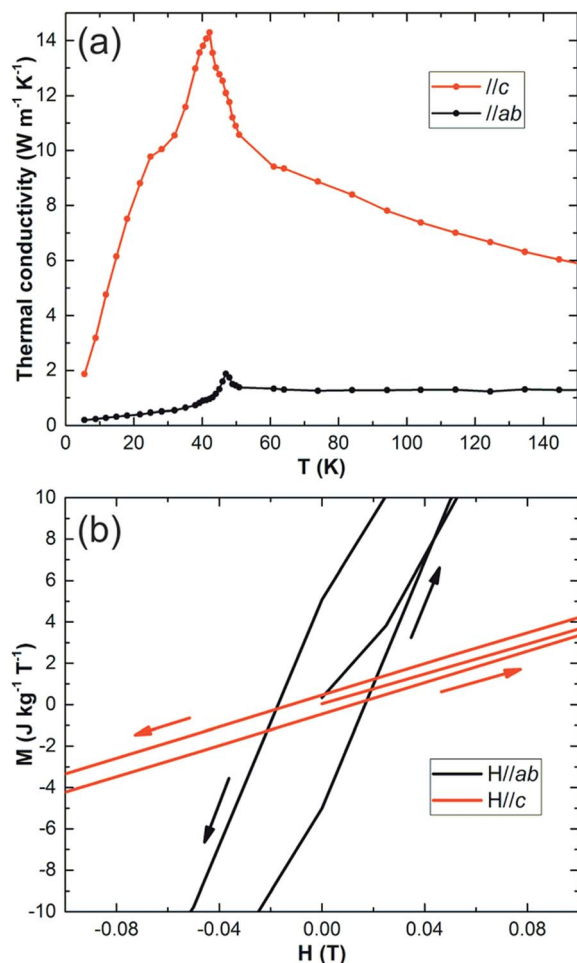


Fig. 4 (a) Variation of thermal conductivity with temperature for gaufreyite along *c* (upper plot) and in the *ab* plane (lower plot). (b) Magnetic hysteresis of gaufreyite at 1.8 K.

(2) Very fast cooling rate due to the magnetic frustration between the chains.

Nevertheless, since previous work²¹ showed that rare earth substituted analogues of gaufreyite can be synthesised, we have examined the effect of increasing the total magnetic spin number by synthesizing $\text{GdCa}_3\text{Mn}_3\text{O}_3(\text{BO}_3)_4$. For this material, even larger entropy changes are observed, especially for large applied fields and lower temperatures: Fig. 5 indicates a change of $20 \text{ J kg}^{-1} \text{ K}^{-1}$ for a ceramic sample of $\text{GdCa}_3\text{Mn}_3\text{O}_3(\text{BO}_3)_4$ for a field of 7 T. Even for polycrystalline materials, and at smaller field, the entropy change is larger than the powder average of the gaufreyite crystal. This behavior means that the magnetic spins of Gd^{3+} and Mn^{3+} are decoupled and each FM MnO_6 chain responds as a giant spin to enhance the total internal field experienced by the paramagnetic Gd^{3+} spins. Although the incorporation of Gd results in a higher entropy change in high fields, the major change observed is the remarkable enhanced entropy change at lower temperatures. In fact we believe that $\text{GdCa}_3\text{Mn}_3\text{O}_3(\text{BO}_3)_4$ is unique in providing an entropy change that is greater than $10 \text{ J kg}^{-1} \text{ K}^{-1}$ for all temperatures below 20 K for a field of 5 T.

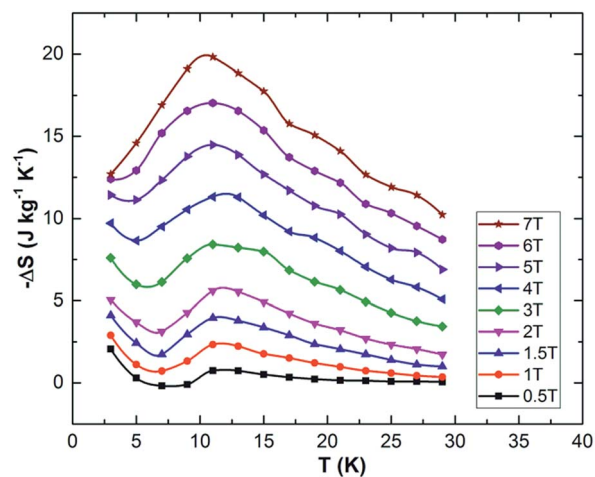


Fig. 5 Entropy changes for $\text{GdCa}_3\text{Mn}_3\text{O}_3(\text{BO}_3)_4$ at fields up to 7 T.

In conclusion, gaufreyite provides excellent MC properties between 10 and 20 K. If even better performance is needed at lower temperatures, the introduction of some Gd can achieve this. We have examined only Mn^{3+} ions and anticipate that the synthesis of materials with similar FM chains could lead to even further enhancements in the MC characteristics of materials with related structures.

Conflicts of interest

There are no conflicts to declare.

Acknowledgements

This project was supported by the National Instrumentation Program (No. 2012YQ120048) of P. R. China and the UK Engineering and Physical Sciences Research Council (EPSRC GR/S2672/01).

Notes and references

- O. Sari and M. Balli, *Int. J. Refrig.*, 2014, **37**, 8–15.
- A. Kitanovski, J. Tušek, U. Tomc, U. Plaznik, M. Ožbolt and A. Poredoš, in *Magnetocaloric Energy Conversion: From Theory to Applications*, Springer International Publishing, Switzerland, 2015.
- B. F. Yu, M. Liu, P. W. Egolf and A. Kitanovski, *Int. J. Refrig.*, 2010, **33**, 1029–1060.
- J. Liu, T. Gottschall, K. P. Skokov, J. D. Moore and O. Gutfleisch, *Nat. Mater.*, 2012, **11**, 620–626.
- I. D. Hepburn, I. Davenport and A. Smith, *Space Sci. Rev.*, 1995, **74**, 215–223.
- T. Numazawa, K. Kamiya, T. Utaki and K. Matsumoto, *Cryogenics*, 2014, **62**, 185–192.
- I. M. Park and S. K. Jeong, *IOP Conf. Series: Materials Science and Engineering*, 2015, vol. 101, p. 012106.
- K. Sakata, E. Mizutani and K. Fukuda, *J. Power Sources*, 2016, **159**, 100–106.



- 9 G. Lorusso, J. W. Sharples, E. Palacios, O. Roubeau, E. K. Brechin, R. Sessoli, A. Rossin, F. Tuna, E. J. L. McInnes, D. Collison and M. Evangelisti, *Adv. Mater.*, 2013, **25**, 4653–4656.
- 10 Y. C. Chen, J. Prokleska, W. J. Xu, J. L. Liu, J. Liu, W. X. Zhang, J. H. Jia, V. Sechovsky and M. L. Tong, *J. Mater. Chem. C*, 2015, **3**, 12206–12211.
- 11 T. Samanta, I. Das and S. Banerjee, *Appl. Phys. Lett.*, 2007, **91**, 152506.
- 12 Z. J. Mo, J. Shen, L. Q. Yan, C. C. Tang, J. Lin, J. F. Wu, J. R. Sun, L. C. Wang, X. Q. Zheng and B.-G. Shen, *Appl. Phys. Lett.*, 2013, **103**, 052409.
- 13 T. Numazawa, K. Kamiya, T. Okano and K. Matsumoto, *Phys. B*, 2003, **329–333**, 1656–1657.
- 14 V. K. Pecharsky and K. A. Gschneidner Jr, *Phys. Rev. Lett.*, 1997, **78**, 4494–4497.
- 15 D. Serantes, V. Vega, W. O. Rosa, V. M. Prida, B. Hernando, M. Pereiro and D. Baldomir, *Phys. Rev. B: Condens. Matter Mater. Phys.*, 2012, **86**, 104431.
- 16 J. W. Sharples, D. Collison, E. J. L. McInnes, J. Schnack, E. Palacios and M. Evangelisti, *Nat. Commun.*, 2014, **5**, 5321.
- 17 M. E. Zhitomirsky, *Phys. Rev. B: Condens. Matter Mater. Phys.*, 2003, **67**, 104421.
- 18 J. Schnack, R. Schmidt and J. Richter, *Phys. Rev. B: Condens. Matter Mater. Phys.*, 2007, **76**, 054413.
- 19 S. S. Sosin, L. A. Prozorova, A. I. Smirnov, A. I. Golov, I. B. Berkutov, O. A. Petrenko, G. Balakrishnan and M. E. Zhitomirsky, *Phys. Rev. B: Condens. Matter Mater. Phys.*, 2005, **71**, 094413.
- 20 R. K. Li and C. Greaves, *Phys. Rev. B: Condens. Matter Mater. Phys.*, 2004, **70**, 132411.
- 21 R. K. Li and C. Greaves, *Phys. Rev. B: Condens. Matter Mater. Phys.*, 2003, **68**, 172403.
- 22 J. Gutzmer and N. J. Beukes, *Ore Geol. Rev.*, 1996, **11**, 405–428.
- 23 M. M. Granger and J. Protas, *C. R. Acad. Sci.*, 1965, **260**, 4553.
- 24 C. Hoffmann, T. Armbruster and M. Kunz, *Eur. J. Mineral.*, 1997, **9**, 7–19.
- 25 V. K. Pecharsky and K. A. Gschneidner Jr, *J. Appl. Phys.*, 1999, **86**, 565–575.
- 26 A. Smith, C. R. H. Bahl, R. Bjørk, K. Engelbrecht, K. K. Nielsen and N. Pryds, *Adv. Energy Mater.*, 2012, **2**, 1288–1318.
- 27 S. Pakhira, C. Mazumdar, R. Ranganathan, S. Giri and M. Avdeev, *Phys. Rev. B*, 2016, **94**, 104414.
- 28 P. Wikus, E. Canavan, S. T. Heine, K. Matsumoto and T. Numazawa, *Cryogenics*, 2014, **62**, 150–152.
- 29 A. M. Aliev, A. B. Batdalov, L. N. Khanov, V. V. Koledov, V. G. Shavrov, I. S. Tereshina and S. V. Taskaev, *J. Alloys Compd.*, 2016, **676**, 601–605.
- 30 T. Numazawa, O. Arai, Q. Hu and T. Noda, *Meas. Sci. Technol.*, 2001, **12**, 2089–2094.

